EFFECT OF VARIABLE VISCOSITY AND HEAT SOURCES ON CONVECTIVE HEAT TRANSFER FLOW OF SWCNT AND MWCNT ROTATING NANOFLUID IN A VERTICAL CHANNEL

B. Sreenivasa Reddy[1] and A. Malleswari[2]

[1]Associate Professor, Department of Applied Mathematics, Yogivemana University, Kadapa, A.P., India, Email : keerthireddybsr@gmail.com Mobile : +91 9440137149

[2]Research Scholar, Department of Applied Mathematics, Yogivemana University, Kadapa, A.P., India, Email : andelamalleswari123@gmail.com

2.1. INTRODUCTION

The Nano fluids can be described as a mixture of nanometer sized particles (diameter less than 100 nm) in the base fluid. The heat/mass transfer analysis in nanofluids has been the topic of extensive research due to intensification of thermal properties in heat transfer processes. The nanoparticles are prepared from copper, aluminium, titanium oxide, gold and the materials that are stable chemically. The inspiration of suspended nanoparticles in a base fluid to increase the thermal conductivity was proposed by Choi [7] about a decade ago. Thereafter, theoretical and experimental investigations on the nanofluid heat transfer property have been conducted by Wang et al. [22], Eastman et al. [9], Buongiorno [6], etc. They have concluded that the thermal conductivity of the base fluid can be dramatically enhanced in the presence of nanoparticles. Besides, there are two models are available to incorporate nanoparticle effect on fluid flow problems namely single phase model and two-phase model. Further, Buongiorno or Tiwari and Das model is used to model the single-phase nanofluid. Two important mechanisms such as Brownian motion and thermophoresis are treated in Buongiorno model. However, in Tiwari and Das model, the effective fluid properties are taken into account. The nanofluids have tremendous applications such as engine cooling, solar water heating, cooling of electronic equipments, cooling of transformer oil, cooling of heat exchanging devices, in chillers, refrigerator–freezers, nuclear reactors, and space vehicles, due to their higher thermal conductivity and convective heat transfer rates.

Rotating flows of nanofluids have also garnered considerable attention. Such studies invoke Coriolice body force terms due to the rotation of the nanofluid. (Mahajan and Arora [13]) considered convective instability in a thin layer of a rotating magnetic nanofluid, considering Brownian diffusion, thermophoresis and magnetophoresis effects.

Using a Chebyshev pseudo spectral numerical method and considering different boundary conditions, they found that for water and ester based magnetic nanofluids, the magnetic field dominates the buoyancy mechanism in fluid layers about 1 mm thick. (Nadeem and Saleem [16]) investigated with a homotopy analysis method (HAM) the transient mixed MHD rotating nanofluid convection on a rotating cone with magnetic field, and considered three different cases where the fluid is rotating and the cone is at rest, the fluid and the cone are rotating with equal angular velocity in the same direction and where only the cone is in rotation. They showed that magnetic field depresses velocity magnitudes and that velocity field is modified significantly depending on the rotation case employed. (Beg et al. [5]) analyzed the transient stagnation-point boundary layer flow of nanofluids from a spinning sphere, using both homotopy and Adomian decomposition methods. Rana et al. [19] studied with a variational finite element algorithm, the transient magneto-hydrodynamic boundary layer flow and heat transfer in an incompressible rotating nanofluid over a stretching continuous sheet, showing that both primary and secondary velocity are strongly retarded with increasing Hartmann (magnetic) number whereas temperature and nanoparticle concentration are enhanced. They also found that greater rotational parameter decelerates both primary and secondary velocity, and reduces temperature and nanoparticle concentration. (Sheikholeslami et al. [20]) used a fourth-order Runge–Kutta method to study magnetohydrodynamic (MHD) nanofluid flow and heat transfer in a rotating parallel plate channel system, considering copper, silver, alumina and titanium oxide nano-particles suspended in water. They showed that Nusselt number is a maximum for the titanium oxide-water nanofluid case whereas it is strongly reduced with increasing magnetic parameter of two types of water-based nanofluids (Cu, Al_2O_3) in a vertical channel and unsteady MHD by Arundati et al[2], Aziz et al. [3], Bagh Ali [4], Hamad and Pop [11], Mohyud-Din et al. [14], Mustafa et al. [15], Sreedevi and Prasada Rao [21].

Dulal and Hiramony [8] analysed the effects of temperature-dependent viscosity and variable thermal conductivity on mixed convective diffusion flow. They found that velocity profile increases while temperature decreases with increase in mixed convection. Gayathri [10] the effect of variable viscosity, activation energy, Brownian motion, Thermophoresison hydromagnetic mixed convective heat and mass transfer flow through a porous medium in a Co-axial cylindrical duct where the boundaries are maintained at temperature Tw and Concentration Cw in the presence of heat generating sources.

Kiran Kumar et al [12] have investigated the effect of thermal radiation on non Darcy hydromagnetic convective heat and mass transfer flow of a water–SWCNT's and MWCNT's nanofluids in a cylindrical annulus with thermo-diffusion and chemical reaction. Patakota Sudarsana Reddy et al[18] have analyzed MHD convective flow of swcnts-water and mwcnts-water nanofluid over a vertical cone with thermal radiation and chemical reaction. Ali et al [1] were experimental investigation on the enhancement of heat transfer by using carbon nanotubes CNT taunit m series.

In this paper we investigate the combined influence of variable viscosity thermal radiation on convective heat transfer flow of swcnt and mwcnt nanofluid in a vertical channel in the presence of heat generating sources. The nonlinear coupled equations governing the flow, heat transfer of nanofluid have been solved by Finite element technique with quadratic interpolation functions. The effect of the velocity, temperature and have been discussed for different parametric variations. The skin friction, rate of heat transfer on the channel walls are numerically evaluated for different variations.

2.2. FORMULATION OF THE PROBLEM:

We consider the steady, three dimensional flow of a nanofluid consisting of a base fluid and small nanoparticles in a vertical porous channel with thermal radiation. A uniform magnetic field of strength Ho is applied normal to the plate. It is assumed that there is no applied voltage which implies the absence of an electric field. The flow is assumed to be in the x-direction which is taken along the plane in an upward direction and z-axis is normal to the plate. Also it is assumed that the whole system is rotating with a constant angular velocity vector $\overline{\Omega}$ about the z-axis. The fluid is assumed to be gray, absorbing emitting but not scattering medium. The radiation heat flux in the x-direction is considered negligible in comparison with that in the z-direction. Due to the fully developed assumption, the flow variables are functions of z and t only. Figure. 1 shows that the problem under consideration and the co-ordinate system.

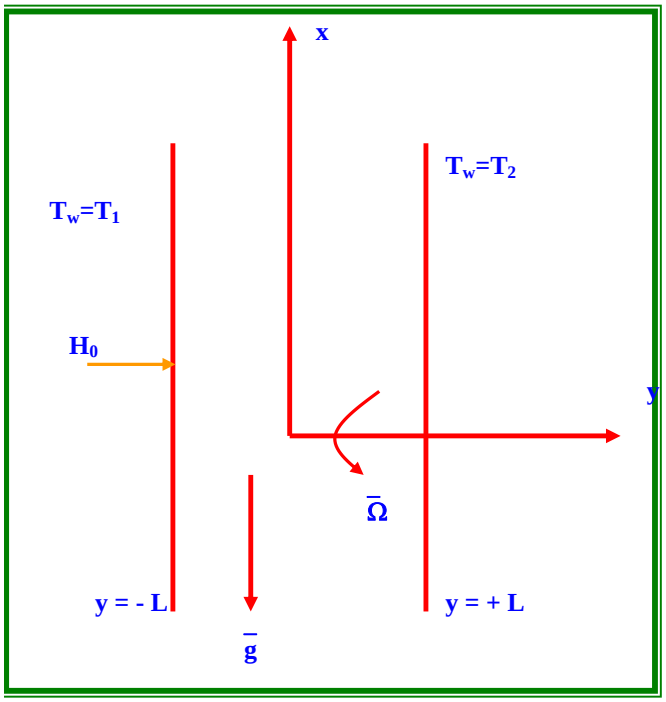

Figure 1 . Schematic diagram of the problem

In the present problem, the following assumptions have been made: The conservation equation of current density $\nabla.\bar{J} = 0$ gives Jz=constant.

Under the above mentioned assumptions, the equation of momentum and thermal energy respectively under Rosseland approximation can be written in dimensional form as :

$$\frac{\partial w}{\partial z} = 0 \qquad (2.2.1)$$

$$\rho_{nf}(w\frac{\partial u}{\partial z} - 2\Omega v) = \frac{\partial}{\partial z}(\mu_{nf}(T)\frac{\partial u}{\partial z}) + (\rho\beta)_{nf} g(T - T_0) - (\sigma_{nf}\mu_e^2 H_o^2)u) \qquad (2.2.2)$$

$$\rho_{nf}(w\frac{\partial v}{\partial z} + 2\Omega u) = \frac{\partial}{\partial z}(\mu_{nf}(T)\frac{\partial v}{\partial z}) - (\sigma\mu_e^2 H_o^2)v) \qquad (2.2.3)$$

$$(\rho C_P)_{nf}(w\frac{\partial T}{\partial z}) = (k_{nf} + \frac{16\sigma^{\bullet} T_0^3}{3\beta_R})\frac{\partial^2 T}{\partial z^2} + Q_H(T - T_0) + \\ +2\mu_{nf}((\frac{\partial u}{\partial z})^2 + (\frac{\partial v}{\partial z})^2) + (\sigma_f \mu_e^2 H_0^2)(u^2 + v^2) \qquad (2.2.4)$$

The boundary conditions are:

$$u(\pm L) = 0 \quad , \quad v(\pm L) = 0, \\ T(-L) = T_1 \ , \quad T(+L) = T_2 \qquad (2.2.6)$$

The properties of the nanofluids are defined as follows:

$$\left.\begin{array}{l} \mu_{nf} = \mu_f / (1-\varphi)^{2.5} \qquad \alpha_{nf} = \dfrac{k_{nf}}{(\rho C_p)_{nf}} \qquad \rho_{nf} = (1-\varphi)\rho_f + \varphi\rho_s \\ (\rho C_p)_{nf} = (1-\varphi)(\rho C_P)_f + \varphi(\rho C_P)_s \qquad (\rho\beta)_{nf} = (1-\varphi)(\rho\beta)_f + \varphi(\rho\beta)_s \\ k_{nf} = \dfrac{k_f(k_s + 2k_f - 2\varphi(k_f - k_s))}{(k_s + 2k_f + 2\varphi(k_f - k_s))}, \sigma_{nf} = (\sigma_f + \dfrac{3(\sigma_f - \sigma_s)\phi}{(\sigma_s + 2\sigma_f)}), \end{array}\right\} (2.2.6)$$

where the subscripts nf, f and s represent the thermo physical properties of the nanofluid, base fluid and the nanosolid particles respectively and ϕ is the solid volume fraction of the nanoparticles. The thermo physical properties of the nanofluid are given in Table 1.

The thermo physical properties of the nanofluids are given in Table 1 (See ***Oztop and Abu-Nada*** [17].

Table – 1 : Physical Properties of nanofluids

Physical properties	Fluid phase (Water)	**Swcnt's**	**Mwcnt's**
C_p(j/kg K)	4179	**425**	**796**
ρ(kg m^3)	997.1	**2600**	**1600**
k(W/m K)	0.613	**6600**	**3000**
βx10^{-5} 1/k)	21	2.0	**2.0**
σ	**0.05**	**10^6**	**10^7**

We consider the solution of equation(2.2.1) as:

$$w = -w_0 \qquad (2.2.7)$$

The dynamic viscosity of the nanofluids is assumed to be temperature dependent as follows:

$$\mu_{nf}(T) = \mu_f Exp(-m(T - T_o)) \qquad (2.2.8)$$

where μ_{nf} is the nanofluid viscosity at the ambient temperature To, m is the viscosity variation parameter which depends on the particular fluid.

We introduce the following dimensionless variables:

$$z' = \frac{z}{L},\ u' = \frac{u}{w_0},\ v' = \frac{v}{w_0},\ \theta = \frac{T - T_1}{T_2 - T_1}, G = \frac{\beta g (T_2 - T_1) L^2}{\mu_f w_o}, B = m(T_2 - T_1),$$
$$S = \frac{w_0 L}{\mu_f},\ M = \frac{\sigma \mu_e^2 H_0^2 L^2}{\rho_f \mu_f},\ Q = \frac{Q_H L^2}{k_f},\ Rd = \frac{4\sigma^{\bullet} T_\infty^3}{\beta_R k_f} \qquad (2.2.9)$$

Equations(2.2.2)-(2.2.4) in the non-dimensional form are

$$0 = \left(\frac{\partial^2 u}{\partial z^2} - B\frac{\partial u}{\partial z}\frac{\partial \theta}{\partial z}\right) + Exp(B\theta)[A_1 A_3(-S\frac{\partial u}{\partial z} - 2Rv) + + A_1 A_4 G\theta - A_1 A_6 M^2 u] \qquad (2.2.10)$$

$$0 = \left(\frac{\partial^2 v}{\partial z^2} - B\frac{\partial v}{\partial z}\frac{\partial \theta}{\partial z}\right) + Exp(B\theta)[A_1 A_3(S\frac{\partial v}{\partial z} - 2Ru) - A_1 A_6 M^2 v] \qquad (2.2.11)$$

$$0 = (1 + \frac{4Rd}{3})\frac{\partial^2 \theta}{\partial z^2} + S\,\mathrm{Pr}\frac{\partial \theta}{\partial z} - Q\theta + Ec\,\mathrm{Pr}\,Exp(-B\theta)[(\frac{\partial u}{\partial z})^2 + (\frac{\partial v}{\partial z})^2] + \qquad (2.2.12)$$
$$+ Ec\,\mathrm{Pr}\,M^2(u^2 + v^2)$$

where

$$A_1 = (1-\varphi)^{2.5} \quad A_2 = \frac{k_{nf}}{k_f}, \quad A_3 = 1 - \varphi + \varphi(\frac{\rho_s}{\rho_f}),\ A_4 = 1 - \varphi + \varphi((\frac{(\rho\beta)_s}{(\rho\beta)_f}), A_5 = 1 - \varphi + \varphi\frac{(\rho C_P)_s}{(\rho C_P)_f},$$
$$A_6 = (1 + \frac{3(1-\sigma)\phi}{(\sigma+2)}), \sigma = \frac{\sigma_s}{\sigma_f} \qquad (2.2.13)$$

The boundary conditions (2.2.5) reduce to

$$u(\pm 1) = 0, v(\pm 1) = 0, \theta(-1) = 0,, \theta(+1) = 1 \qquad (2.2.14)$$

Method of solutions:

2.3. FINITE ELEMENT ANALYSIS

The finite element analysis with quadratic polynomial approximation functions is carried out along the axial distance across the vertical channel. The behavior of the velocity, temperature profiles has been discussed computationally for different variations in governing parameters. The Galerkin method has been adopted in the variational formulation in each element to obtain the global coupled matrices for the velocity, temperature and concentration in course of the finite element analysis.

Choose an arbitrary element e_k and let u^k, v^k θ^k be the values of u, v,θ in the element e_k. We define the error residuals as

$$E_u^k = \frac{d}{dz}\left(\frac{du^k}{dz}\right) + -B\frac{du^k}{dz}\frac{d\theta^k}{dz} + e^{B\theta}[A_1 A_4 G(\theta^k) - Su^k - 2Rv^k + A_1 A_6 M^2 u^k] \quad (2.3.1)$$

$$E_v^k = \frac{d}{dz}\left(\frac{dv^k}{dz}\right) - B\frac{dv^k}{dz}\frac{d\theta^k}{dz} + e^{B\theta}[-Sv^k - 2Ru^k + A_1A_6M^2v^k] \qquad (2.3.2)$$

$$E^k{}_\theta = \frac{A_2}{\Pr}\frac{d}{dz}\left(\frac{d\theta^k}{dz}\right) - S\Pr\theta^k A_5 u^k - Q\theta^k + Ece^{-B\theta}[(\frac{du^k}{dz})^2 + (\frac{dv^k}{dz})^2] +$$

$$+ EcM^2((u^k)^2 + (v^k)^2) \qquad (2.3.3)$$

where u^k, v^k, θ^k are values of u,v, θ in the arbitrary element e_k. These are expressed as linear combinations in terms of respective local nodal values.

$$u^k = u_1^k\psi_1^k + u_2^k\psi_1^k + u_3^k\psi_3^k,$$
$$v^k = v_1^k\psi_1^k + v_2^k\psi_1^k + v_3^k\psi_3^k$$
$$\theta^k = \theta_1^k\psi_1^k + \theta_2^k\psi_2^k + \theta_3^k\psi_3^k \qquad (2.3.4)$$

where ψ_1^k, ψ_2^k --------- etc are Lagrange's quadratic polynomials.

Galarkin's method is used to convert the partial differential Equations (2.3.1) – (2.3.4) into matrix form of equations which results into 3x3 local stiffness matrices. All these local matrices are assembled in a global matrix by substituting the global nodal values and using inter element continuity and equilibrium conditions. The resulting global matrices have been solved by iterative procedure until the convergence i.e $|u_{i+1}-u_i|<10^{-6}$ is obtained.

2.4. DISCUSSION OF THE NUMERICAL RESULTS:

In this Analysis, we explore the combined influence of variable viscosity on convective heat transfer flow of a rotating nanofluid confined in a vertical channel bounded by flat walls. The non-linear coupled equations governing the flow, heat and mass transfer have been solved by fourth order Runge-kutta shooting technique. The velocity, temperature have been analyzed numerically for different variation of G,M,R,K,B, S,Q,Rd,Ec,ϕ and Pr are presented in fig.2-12 for different Swcnt and Mwcnt nanofluids.

Figs.2a-2c demonstrate the variation of velocities, temperature with Grashof number (G). From the profiles we note that the velocity components, temperature experience an enhancement in Gr. The values of the axial velocity (f ′) in Swcnt are relatively greater than the values in Mwcnt while a reversed effect is noticed in case of secondary velocity (g). The values of temperature in Swcnt are greater than those in Mwcnt.

The effect of magnetic field M on f ′ ,g,θ is shown in fig.3a-3c. It is from the profiles we notice that both the velocity components, experience retardation for higher values of magnetic parameter M. It is due to the fact that the presence of the magnetic field produces a force which decays the velocity components in the flow region. The values of velocities components in Swcnt are lesser than those in Mwcnt (fig.3a-3b). From figures 3c, we find that higher the Lorentz force, larger the temperature.

Fig. 4a-4d represent f ′,g,θ with rotation parameter (R). From the profiles we note that higher the coriolice force smaller the axial velocity and larger the secondary velocity (g),From the graphs, we note that the values of f ' in Swcnt are relatively greater than those in Mwcnt while a reversed effect is noticed in case of secondary velocity (g)(figs.4a-4b).

From figs.4c, we observe that the temperature reduces with increasing values of rotation parameter(R). This is due to the fact that increase in R leads to decay in thermal boundary layer and growth in solutal boundary layer .The values of temperature in Swcnt are greater than those in Mwcnt.

Fig.5a-5c investigate the behavior of f ′,g,θ with porous permeability parameter (K). From the velocity profiles, we find that the axial velocity (f ') and temperature(θ) depreciate while secondary velocity(g) enhance with increasing values of porous permeability parameter (K). Also the values of velocities in Swcnt are smaller than those in Mwcnt. The values of temperature in Swcnt are greater than those in Mwcnt

Fig.6a-6c demonstrate the influence of variable viscosity on f ',g,θ. From the profiles we find that higher the values of viscosity parameter (β) we notice a depreciation in axial velocity(f ') and enhancement in secondary velocity(g) and temperature (θ). From the profiles we know that the values of g,θ in Swcnt are lesser than those in Mwcnt. while an opposite effect is observed in the behavior of axial velocity (f ').

Fig.7a-7c, represent the variation of f ',g,θ with suction parameter (S). From the profiles we know that the secondary velocity, temperature experience depreciation with increasing values of S while the axial velocity enhances with S in the entire flow region .Also the values of velocities in Swcnt are greater than those in Mwcnt while a reverse effect is observed in the behavior of θ.

Fig.8a-8c represent the effect of heat generating source (Q) on f ', g, θ. From the profiles we find that the axial velocity, while temperature reduces in both Swcnt and Mwcnt with increase in values of heat generating source (Q>0). An increase in Q>0 reduces the secondary velocity(g) in Swcnt and enhances in Mwcnt.

Figs. 9a-9c demonstrate the behavior of f ',g,θ with thermal radiation parameter (Rd). From the profiles we note that higher the thermal Radiation parameter larger the velocity , temperature in the flow region. Also, the values of velocities and temperature in Swcnt are much greater than those in Mwcnt.

The effect of dissipation (Ec) on the flow variables can be seen in 10a-10c. From the profiles we find that higher the dissipation larger the magnitude of velocity and temperature. The values of velocities, temperature in Swcnt are greater than those in Mwcnt.

Fig.11a-11c , demonstrate the influence of nanoparticle concentration (ϕ) on flow variables. From the profiles we find that as the nanoparticle volume fraction increases the nanofluid primary and secondary velocity components, temperature decrease in the boundary layer. These figures illustrate this agreement with the physical behavior when the volume of nanoparticles increases, the thermal conductivity and thermal boundary layer thickness is decreasing. We also notice that nanofluid velocity components in the case of Swcnt are relatively greater than those of Mwcnt. Fig.11c-11c , show the variation of θ with ϕ. It can be seen from the profiles that an increase in ϕ reduces the temperature in the boundary layer due to the fact that the thickness of thermal and solutal boundary layer decays with increasing values in ϕ. Also the values of θ in the case of Swcnt are relatively lesser than those in Mwcnt.

Fig.12a-12c show the variation of f ',g,θ with Prandtl number (Pr). From the profiles we find that lesser the thermal diffusivity smaller the velocity and temperature in the boundary layer. The values of velocity components in Swcnt are relatively greater than those in Mwcnt while a reversed behavior is noticed in the temperature.

The skin friction component τ_x at $\eta = -1$, increases with Grashof number/Suction parameter/Radiation parameter/Eckert number/naboparticle volume fraction(ϕ) and reduces with increase in rotation parameter(R) in both Swcnt and Mwcnt. An increase in magnetic parameter/porous parameter/ rotation parameter/ heat source parameter/Prandtl number, reduces τ_x in Swcnt and enhances in Mwcnt, at $\eta=-1$, τ_x enhances with G and reduces with S in both Swcnt and Mwcnt. An increase in M/K/B/ϕ/Pr, reduces τ_x in Swcnt and enhances in Mwcnt. Increasing values of Q/Rd/Ec/R enhance τ_x in Swcnt and reduces it in Mwcnt.

The skin friction component τ_y at $\eta =-1$, enhances with G/M/R/B and reduces with increase in Pr. An increase in Q/ϕ, reduces τ_y in Swcnt and enhances in Mwcnt. Increasing values of S/Rd/Ec enhances τ_y in Swcnt and reduces it Mwcnt at $\eta=-1$,τ_y enhances with G/M/R/B and reduces with K/Q/ϕ/Pr .An increase in Suction parameter (S) reduces τ_y in Swcnt and enhances in Mwcnt. Increase in values of Rd/Ec leads to an enhancement in τ_y in Swcnt and depreciation in Mwcnt.

The rate of heat transfer Nu (Nusselt number) at $\eta=-1$ enhances with increase in porous parameter K/ Suction parameter S/ heat source Q and reduces with increase in G/Rd/Ec. Higher the coriolice force(R) , smaller the Nu in Swcnt and larger Nu in Mwcnt. Increase in values of magnetic parameter M/ viscosity B /ϕ/Pr enhances Nu in Swcnt and reduces in Mwcnt at $\eta=+1$,Nu increases with increase in G/S/Rd/Ec and reduces with M/Q/ϕ/Pr. Increase in rotation parameter (R) reduces Nu in Swcnt and enhances in Mwcnt while an opposite effect is observed with increase in viscosity parameter(B) at $\eta=+1$.

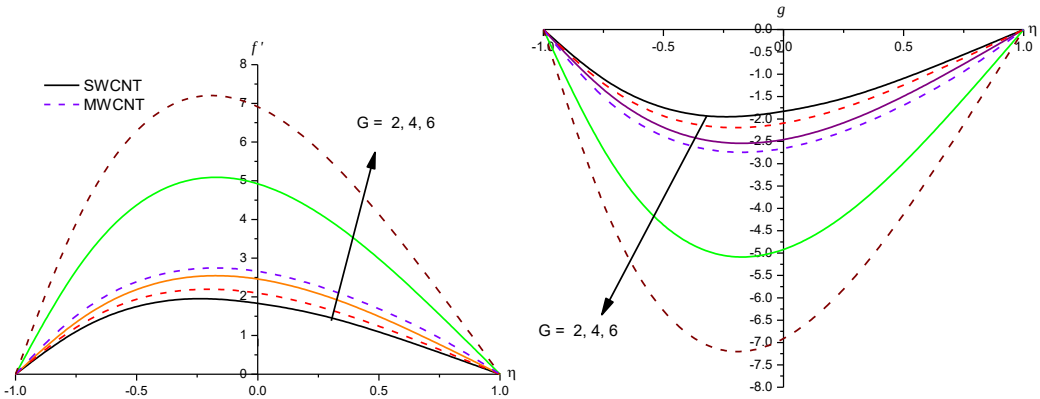

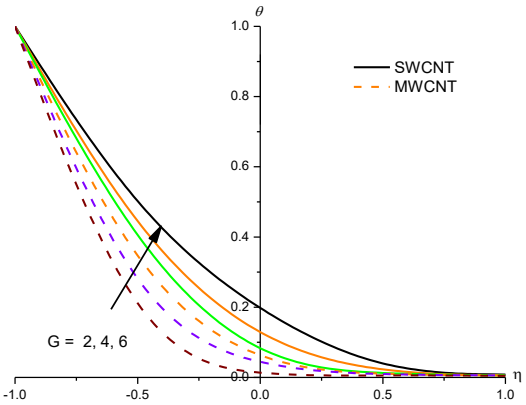

Fig.2 : Variation of [a] Axial velocity(f'), [b] Secondary velocity[g], [c] Temperature(θ) with G

M=0.5, R=0.25, K=0.2, B=0.25, S=0.2, Q=2, Rd=0.5, Ec=0.05, ϕ=0.05, Pr=0.71

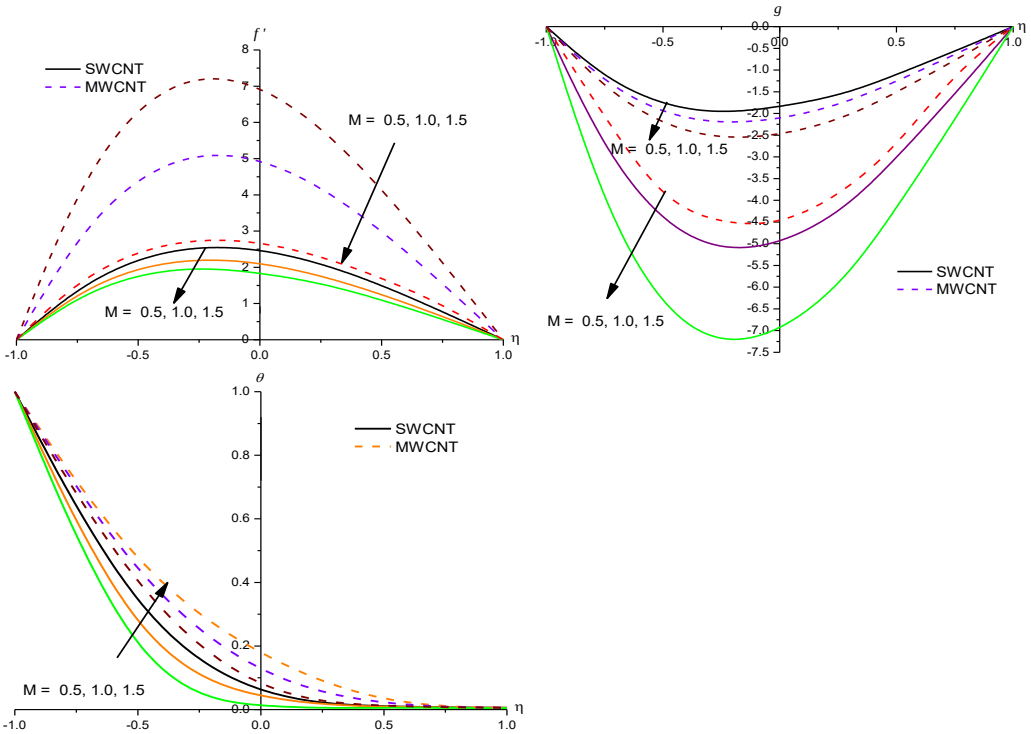

Fig.3 : Variation of [a] Axial velocity(f'), [b] Secondary velocity[g], [c] Temperature(θ) with M

G=2, R=0.25, K=0.2, B=0.25, S=0.2, Q=2, Rd=0.5, Ec=0.05, ϕ=0.05, Pr=0.71

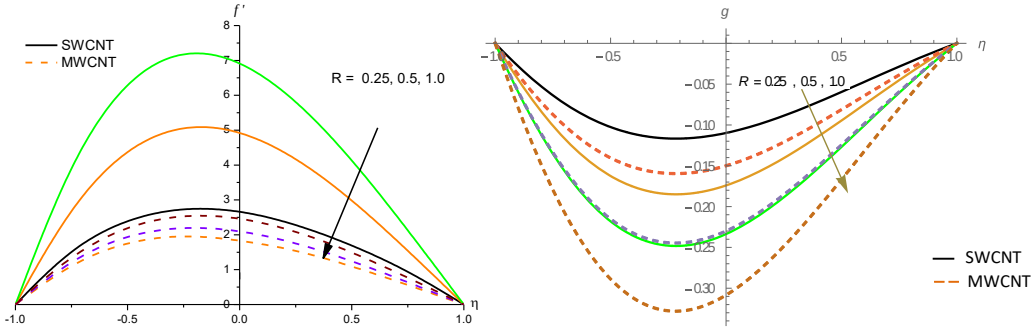

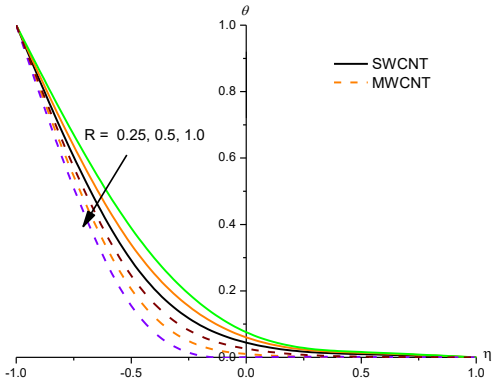

Fig.4 : Variation of [a] Axial velocity(f'), [b] Secondary velocity[g], [c] Temperature(θ) with R

G=2,M=0.5, K=0.2, B=0.25, S=0.2, Q=2, Rd=0.5, Ec=0.05, ϕ=0.05, Pr=0.71

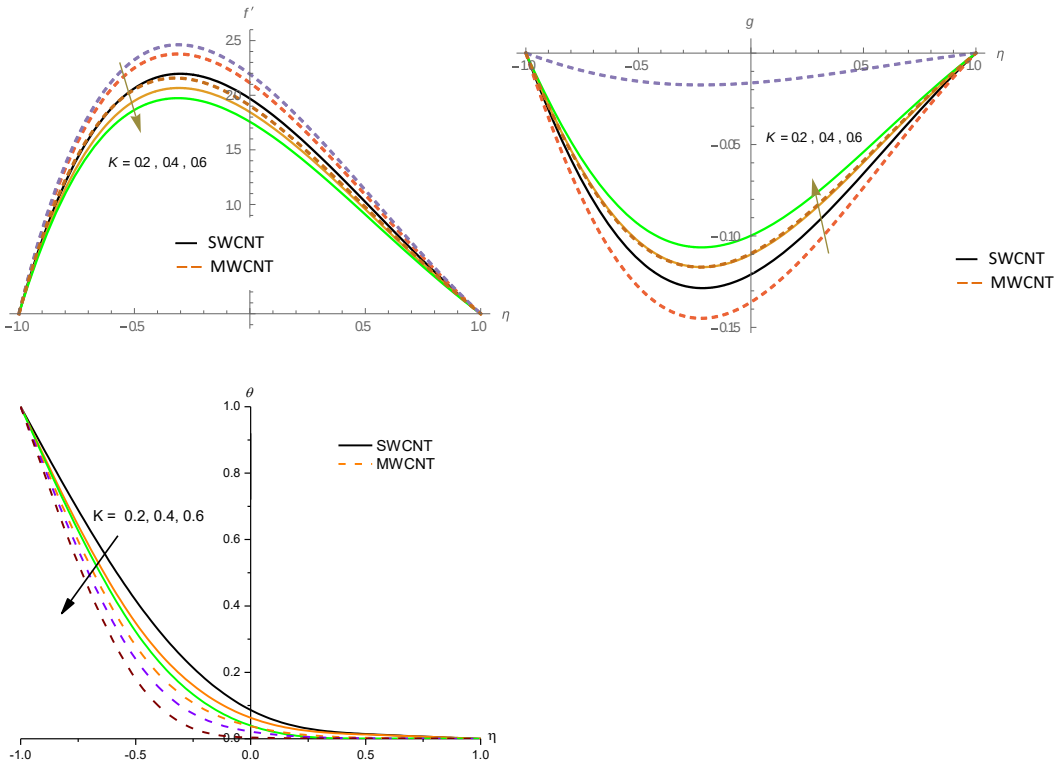

Fig.5 : Variation of [a] Axial velocity(f'), [b] Secondary velocity[g], [c] Temperature(θ) with K

G=2,M=0.5, R=0.25, B=0.25, S=0.2, Q=2, Rd=0.5, Ec=0.05, ϕ=0.05, Pr=0.71

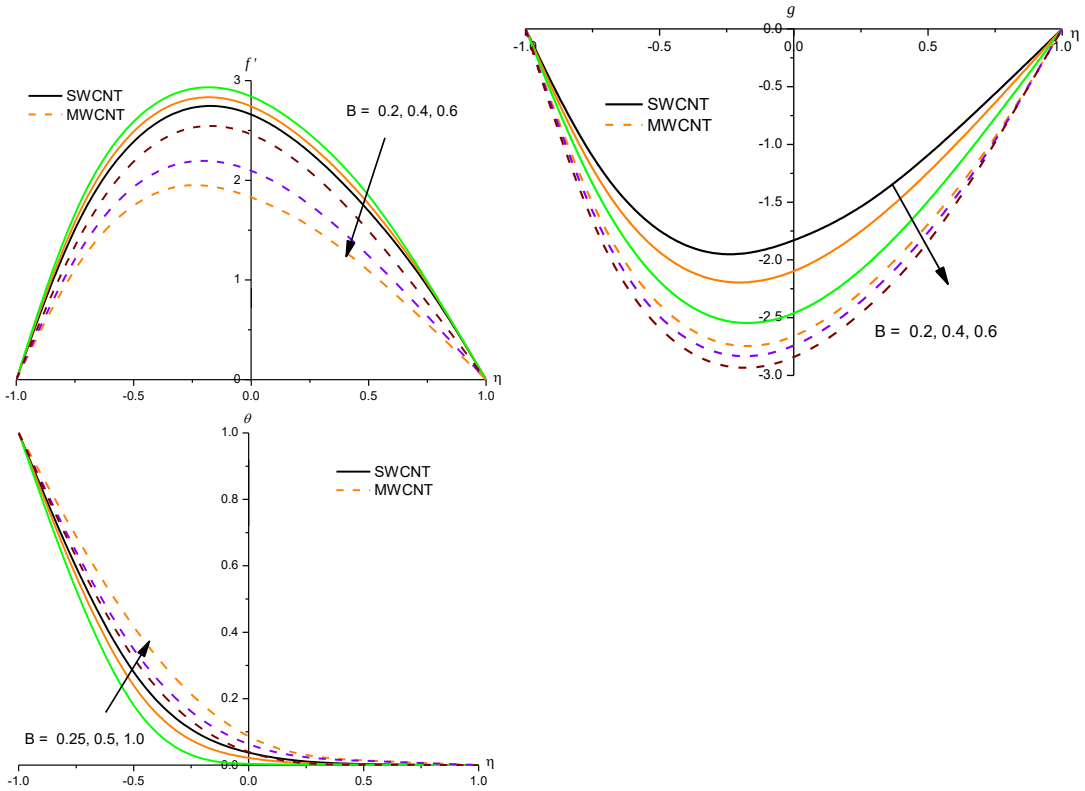

Fig.6 : Variation of [a] Axial velocity(f'), [b] Secondary velocity[g], [c] Temperature(θ) with B

G=2,M=0.5, R=0.25, K=0.2, S=0.2, Q=2, Rd=0.5, Ec=0.05, ϕ=0.05, Pr=0.71

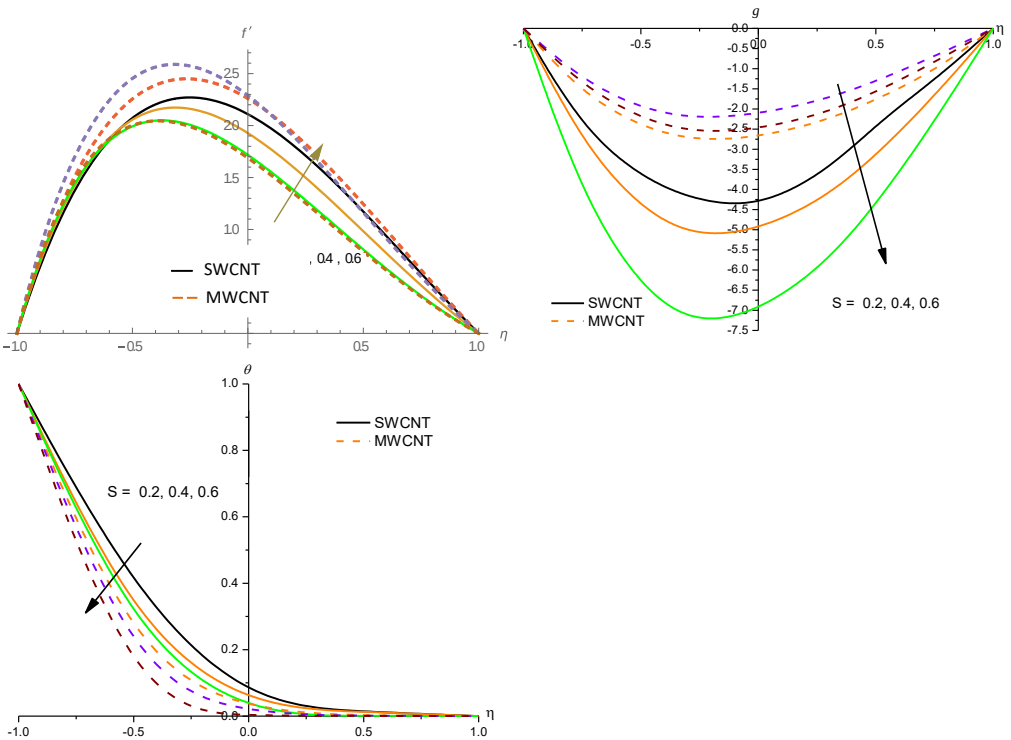

Fig.7 : Variation of [a] Axial velocity(f'), [b] Secondary velocity[g], [c] Temperature(θ) with S

G=2,M=0.5, R=0.25, K=0.2, B=0.25, Q=2, Rd=0.5, Ec=0.05, ϕ=0.05, Pr=0.71

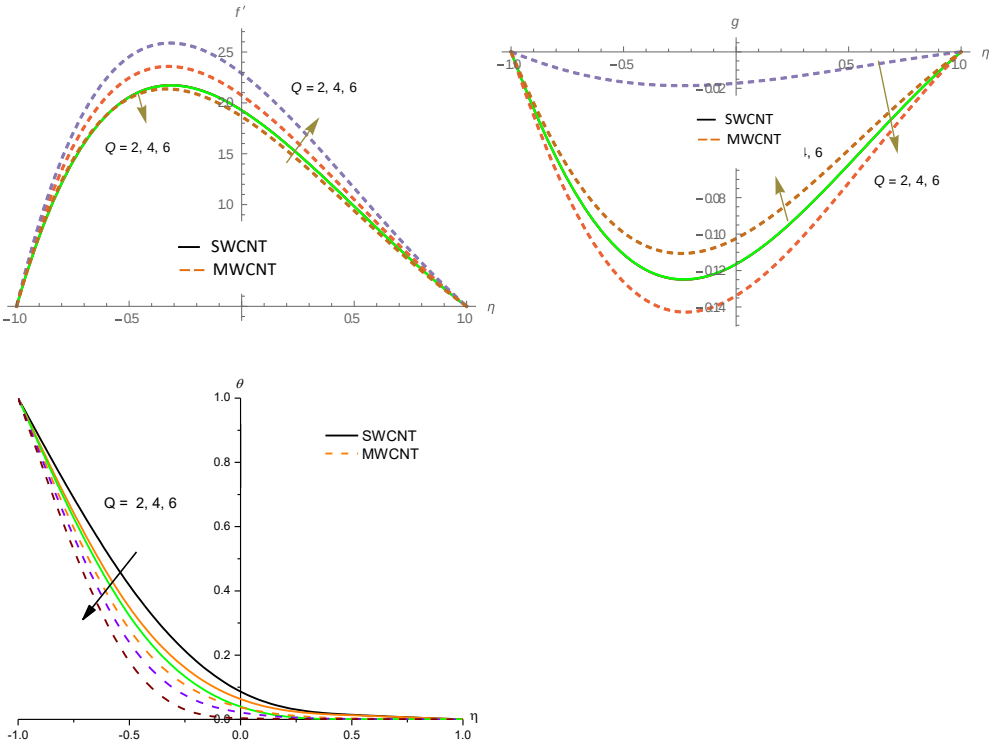

Fig.8 : Variation of [a] Axial velocity(f'), [b] Secondary velocity[g], [c] Temperature(θ) with Q

G=2,M=0.5, R=0.25, K=0.2, B=0.25, S=0.2, Rd=0.5, Ec=0.05, ϕ=0.05, Pr=0.71

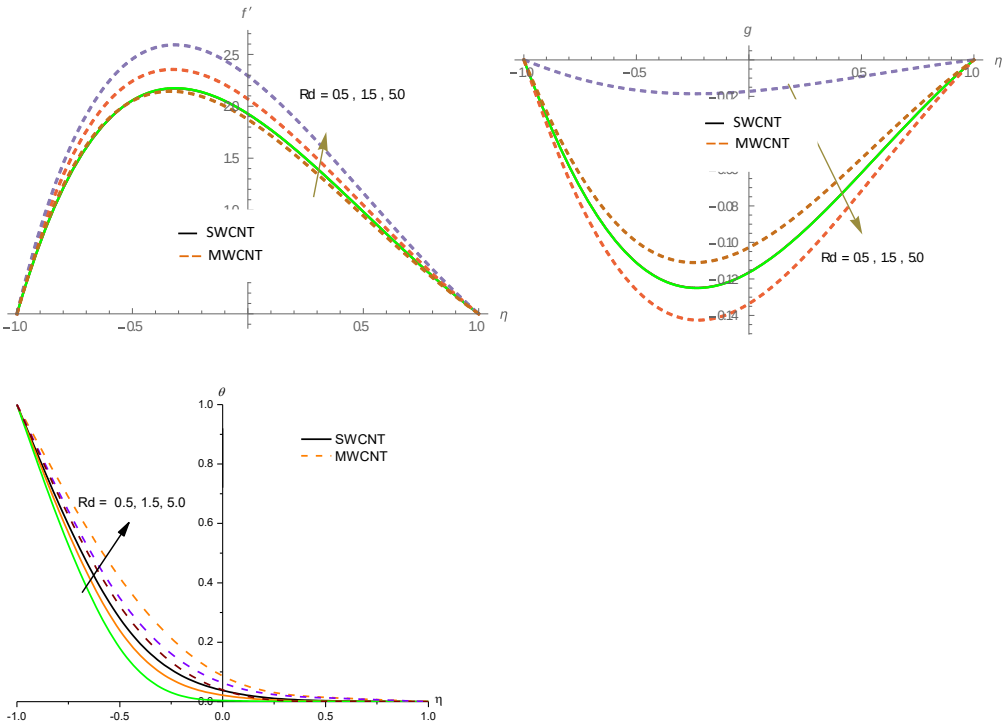

Fig.9 : Variation of [a] Axial velocity(f'), [b] Secondary velocity[g], [c] Temperature(θ) with Rd

G=2,M=0.5, R=0.25, K=0.2, B=0.25, S=0.2, Q=2, Ec=0.05, ϕ=0.05, Pr=0.71

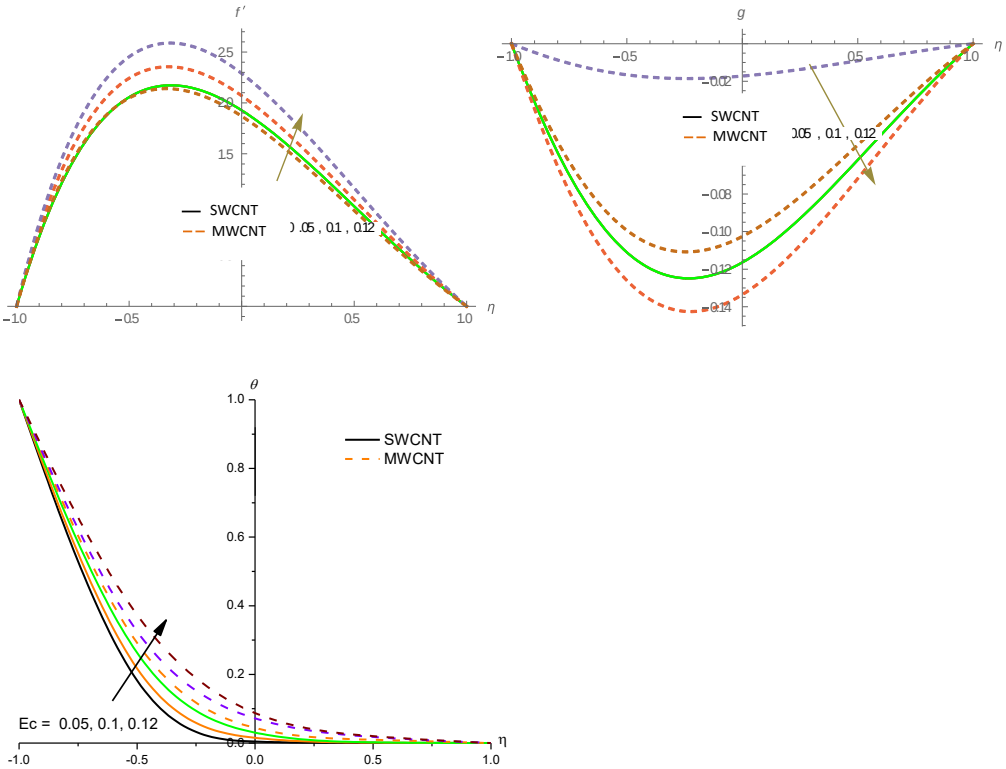

Fig.10 : Variation of [a] Axial velocity(f'), [b] Secondary velocity[g], [c] Temperature(θ)with Ec

G=2,M=0.5, R=0.25, K=0.2, B=0.25, S=0.2, Q=2, Rd=0.5, ϕ=0.05, Pr=0.71

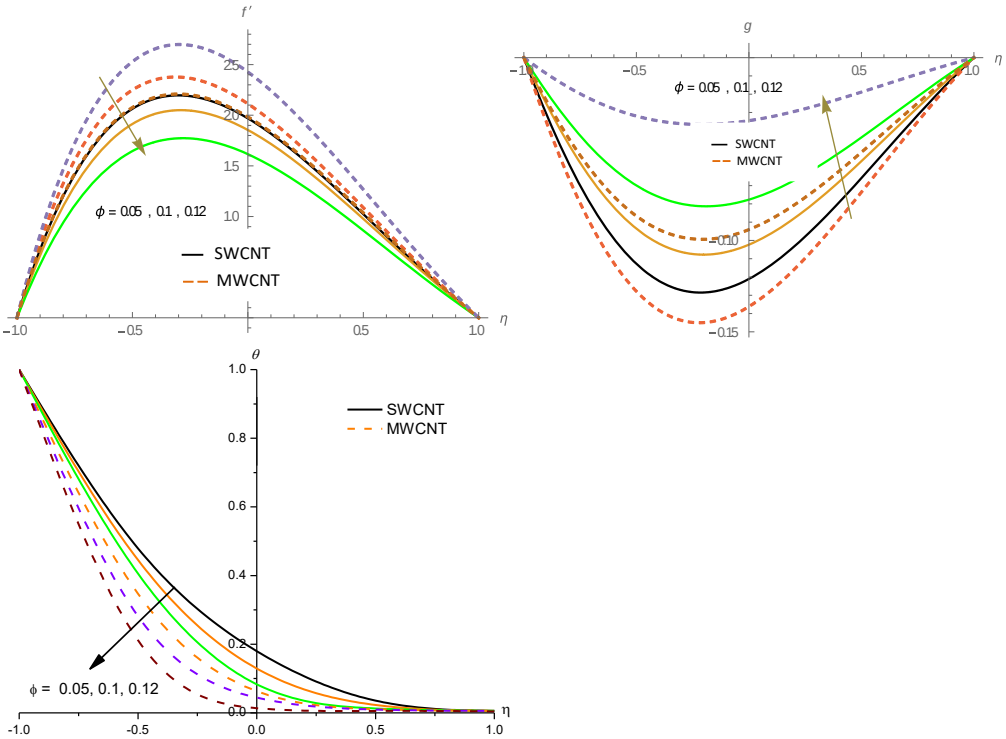

Fig.11 : Variation of [a] Axial velocity(f'), [b] Secondary velocity[g], [c] Temperature(θ) with ϕ

G=2,M=0.5, R=0.25, K=0.2, B=0.25, S=0.2, Q=2, Rd=0.5, Ec=0.05, Pr=0.71

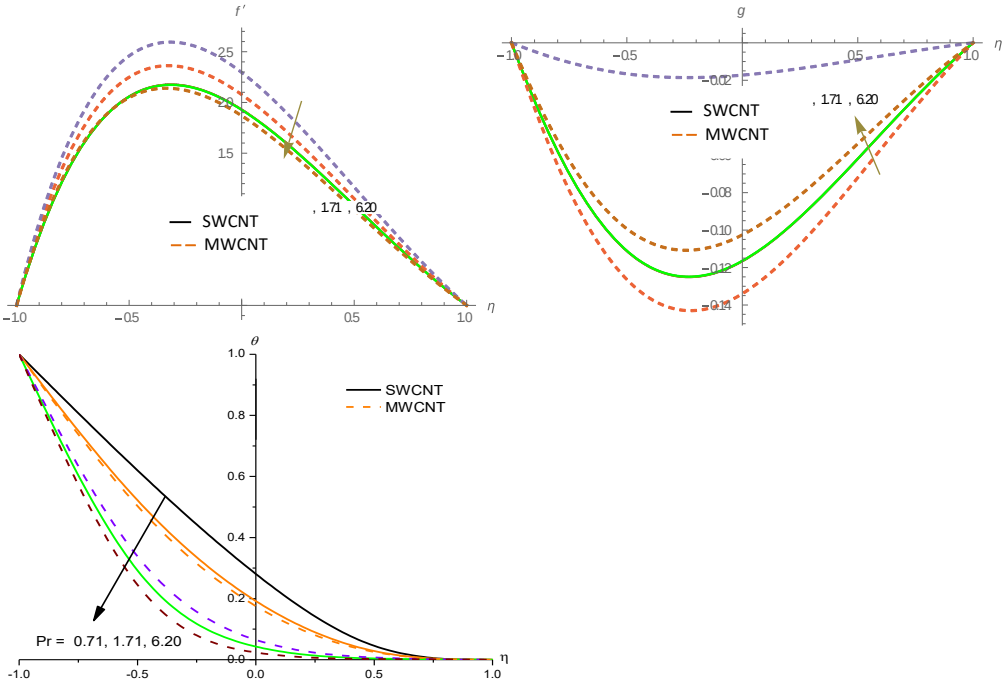

Fig.12 : Variation of [a] Axial velocity(f'), [b] Secondary velocity[g], [c] Temperature(θ) with Pr

G=2,M=0.5, R=0.25, K=0.2, B=0.25, S=0.2, Q=2, Rd=0.5, Ec=0.05, ϕ=0.05

Table 2 : Skin friction ($\tau_{x,z}$), Nusselt number (Nu) at $\eta = -1$ with Swcnt and Mwcnt water nanofluids

Parameter		Swcnt-Water nanofluid			Mwcnt-Water nanofluid		
		τx(-1)	τy(-1)	Nu(-1)	τx(-1)	τy(-1)	Nu(-1)
G	2	7.57134	-0.325859	0.502483	8.33555	-0.444464	0.505408
	4	15.1424	-0.673707	0.502368	16.9104	-0.744189	0.505125
	6	22.7163	-1.010733	0.502175	25.3728	-1.116745	0.504626
M	0.5	7.06699	-0.297172	0.502433	9.48771	-0.728704	0.505318
	1.0	6.79846	-0.482339	0.502478	9.68823	-0.897803	0.505281
	1.5	6.54	-	0.502	10.04	-	0.505

		752	0.686527	482	17	1.233352	215
K	0.2	7.57134	-0.325859	0.502483	8.45374	-0.372001	0.505423
	0.4	7.23691	-0.297885	0.502488	8.67378	-0.324902	0.505416
	0.6	6.99651	-0.271558	0.502491	7.87577	-0.303025	0.505441
R	0.25	7.06699	-0.297172	0.50249	9.05513	-0.407781	0.505504
	0.50	7.05289	-0.470195	0.50240	9.02295	-0.625299	0.505405
	1.00	7.02997	-0.631174	0.50233	8.97768	-0.838958	0.505406
Rd	0.5	7.68897	-0.328744	0.502484	8.58739	-0.367829	0.505425
	1.5	7.69232	-0.328939	0.501381	9.22435	-0.349508	0.503005
	5.0	7.69429	-0.329054	0.500731	9.41384	-0.298561	0.501603
Ec	0.05	7.68897	-0.328744	0.502484	8.58739	-0.367829	0.505425
	0.10	7.68908	-0.328765	0.502458	9.21602	-0.349448	0.505323
	0.12	7.68928	-0.328772	0.502409	10.0299	-0.297982	0.505281
Q	2	7.69246	-0.328942	0.501334	8.59565	-0.368362	0.502899
	4	7.68	-	0.502	9.215	-	0.505

		897	0.328744	484	61	0.049445	405
	6	7.68556	-0.328545	0.503633	9.99492	-0.297554	0.507963
S	0.2	7.11362	-0.309287	0.502373	7.92948	-0.342816	0.505189
	0.4	7.68897	-0.328744	0.502484	8.21561	-0.329445	0.505405
	0.6	8.16984	-0.332293	0.502599	8.55161	-0.307156	0.505683
B	0.25	7.57134	-0.325859	0.502483	8.45374	-0.372001	0.505423
	0.50	7.56992	-0.349799	0.502486	8.77569	-0.382029	0.505403
	1.00	7.56916	-0.362534	0.502493	8.45354	-0.398853	0.505393
ϕ	0.05	7.57134	-0.325859	0.502483	8.45374	-0.372001	0.505423
	0.10	7.90162	-0.265453	0.502541	9.20656	-0.092002	0.50549
	0.12	5.84565	-0.195291	0.502597	7.65021	-0.247441	0.505619
Pr	0.71	7.69596	-0.329148	0.500214	8.60393	-0.368909	0.500455
	1.71	7.69466	-0.329075	0.500621	9.23058	-0.049554 3	0.501327
	6.20	7.68897	-0.328744	0.502484	8.00234	-0.297947	0.505442

Table 3 : Skin friction ($\tau_{x,z}$), Nusselt number (Nu) at $\eta = +1$ with Swcnt and Mwcnt water nanofluids

Parameter		Swcnt-Water nanofluid			Mwcnt-Water nanofluid		
		τx(+1)	τy(+1)	Nu(+1)	τx(+1)	τy(+1)	Nu(+1)
G	2	-1.77092	0.114679	0.498656	-1.83257	0.152186	0.497088
	4	-3.54175	0.237715	0.498735	-3.74597	0.254718	0.497278
	6	-5.31373	0.356642	0.498866	-5.62199	0.382266	0.497611
M	0.5	-1.59526	-0.297172	0.502498	-1.41843	-0.728704	0.505318
	1.0	-1.50312	-0.482339	0.502478	-2.22535	-0.897803	0.505281
	1.5	-1.45678	-0.686527	0.502472	-2.29432	-1.233356	0.505215
K	0.2	-1.77094	0.114679	0.502499	-1.87237	0.127321	0.497078
	0.4	-1.65385	0.104049	0.502497	-1.74708	0.115209	0.497083
	0.6	-1.57049	0.094083	0.502492	-1.67843	0.101842	0.497123
R	0.25	-1.59526	0.103797	0.498652	-2.07703	0.140582	0.497092
	0.50	-1.58991	0.164644	0.498651	-2.06508	0.215466	0.497092
	1.00	-1.58122	0.220898	0.498649	-2.04826	0.288887	0.497122
Rd	0.5	-1.66573	0.105182	0.498655	-1.76553	0.123971	0.497276
	1.5	-1.66709	0.105254	0.499252	-1.66406	0.105375	0.498381
	5.0	-1.66788	0.105296	0.499604	-1.59143	0.091170	0.499134
Ec	0.05	-1.66573	0.105182	0.498655	-1.76553	0.123971	0.497076
	0.1	-1.66578	0.105184	0.498673	-1.66077	0.101353	0.497144
	0.12	-1.66586	0.105189	0.498706	-1.58705	0.090965	0.497169
Q	2	-1.66709	0.105254	0.499236	1.76875	0.124182	0.498335
	4	-1.66573	0.105182	0.498655	-1.66061	0.115352	0.497097
	6	-1.66438	0.105109	0.498082	-1.58386	0.090806	0.495818
S	0.2	-2.19309	0.153396	0.502373	-2.31789	0.180987	0.505189
	0.4	-1.66573	0.105182	0.502484	-1.96061	0.215352	0.505405
	0.6	-1.24044	0.068169	0.502599	-1.20329	0.059948	0.505683
B	0.25	-1.77095	0.114679	0.502483	-1.87237	0.127321	0.505423
	0.50	-1.77035	0.123783	0.502487	-1.98468	0.129844	0.505203
	1.00	-1.77006	0.128635	0.502489	-2.08723	0.137267	0.505423
ϕ	0.05	-1.77097	0.114679	0.498656	-1.87237	0.127321	0.497078
	0.10	-1.71534	0.100298	0.498601	-2.20053	0.122926	0.497004
	0.12	-1.53428	0.078485	0.498547	-2.81523	0.111314	0.496894
Pr	0.71	1.66853	0.105338	0.499888	-1.77213	0.124401	0.499765
	1.71	-1.66803	0.105304	0.499667	-1.96653	0.105391	0.499296
	6.20	-1.66573	0.105182	0.498655	-2.08679	0.090947	0.497064

CONCLUSIONS:

In this analysis wee analyze the impact of variable viscosity, activation energy on MHD convective heat transfer flow of a rotating Nano fluid in a vertical channel bounded by flat walls in the presence of heat generating sources. By using Finite element technique with quadratic interpolation functions the non-linear, coupled equations governing the flow phenomenon has been analyzed. The velocity, temperature have discussed for different parametric variations. The rate of heat and mass transfer are evaluated for different variations. The conclusions of the analysis are:

1. Increase in Grashof number(Gr) enhances the velocity components, temperature and reduces the nanoconcentrtion in both Swcnt and Mwcnt nanofluids. The skin friction components grows at $\eta=\pm1$ with Gr. Nusselt number enhances at the left wall and reduces at the right wall.

2. Higher the Lorentz force smaller the velocity components, enhances the temperature in both nanofluids. Skin friction components($\tau x,\tau y$) reduces in Swcnt nanofluid and enhances in Mwcnt nanofluids at both the walls.Nu reduces with M at $\eta=1$.

3. An increase in rotation parameter(R) reduces the primary velocity, temperature and enhances secondary velocity in both types of nanofluids.τx reduces , τy enhances in Swcnt nanofluid with increase in R. Nu reduces in Swcnt nanofluid and enhances in Mwcnt nanofluid with rising values of R at both the walls at $\eta=\pm1$.

4. The primary velocity reduces, while the secondary velocity, temperature enhances with increasing values of viscosity parameter(B). Skin friction component (τx) reduces in Swcnt and enhances in Mwcnt nanofluids at $\eta=\pm1$. τy enhances at both walls in both types of nanofluids with B. Nu enhances in Swcnt and reduces in Mwcnt nanofluids at $\eta=\pm1$.

5. Higher the thermal radiation (Rd)/dissipation(Ec), larger the velocities, temperature in Swcnt and Mwcnt nanofluids. Skin friction enhance with Rd and Ec at $\eta=-1$ in both types of nanofluids. An increase Rd and Ec reduces Nu at the left wall and enhances at the right wall.

6. An increase nanoparticle volume fraction (ϕ) depreciates velocities, temperature in the entire flow region. Skin friction(τx) enhance with ϕ at $\eta=-1$ in both types of nanofluid while at $\eta=+1$, τy reduces in Swcnt nanofluid and enhances in Mwcnt nanofluid with increase in ϕ.Nu reduces with ϕ at $\eta=1$ in Swcnt and Mwcnt nanofluids while at $\eta=-1$,Nu enhances in Swcnt nanofluid, reduces in Mwcnt nanofluid. Sh reduces with ϕ in Swcnt and enhances in Mwcnt nanofluid at $\eta=-1$ with ϕ.

7. The primary velocity enhance, secondary velocity, temperature reduce with increase in heat generating source. Skin friction components reduces in swcnt and enhances in Mwcnt nanofluids with Q at both walls. Nu enhances, with higher values of Q at $\eta=\pm1$ in both types of nanofluids.

REFERENCES

[1]. Ali A J, Jaber H J, Habeeb L J and Tugolukov E N :Experimental investigation on the enhancement of heat transfer by using carbon nanotubes CNT taunit m series, Materials Science and Engineering, **791,** (2020) 012003, doi:10.1088/1757-899X/791/1/012003

[2]. Arundhati V, Chandra Sekhar K.V., Prasada Rao D.R.V. : Thermal Radiation and Thermodiffusion Effect on Convective Heat and Mass Transfer Flow of a Rotating Nanofluid in a Vertical Channel, *International Conference on Numerical Heat Transfer & Fluid Flow* (NHTFF18), National Institute of Technology (NIT) Warangal, TS, India on Jan 19-21, (2018); *Numerical Heat Transfer and Fluid Flow*: Select Proceedings of NHTFF 2018 (Springer) pp.73-81. https://DOI.org/10.1007/978-981-13-1903-7_10

[3]. Aziz, A.; Khan, W.A.; Pop, I. Free convection boundary layer flow past a horizontal flat plate embedded in porous medium filled by nanofluid containing gyrotactic microorganisms. *Int. J. Therm. Sci.* (2012), 56, 48–57.

[4]. Bagh Ali, Rizwan Ali Naqvi, Yufeng Nie, Shahid Ali Khan, Muhammad Tariq Sadiq, Ateeq Ur Rehman and Sohaib Abdal : Variable Viscosity Effects on Unsteady MHD an Axisymmetric Nanofluid Flow over a Stretching Surface with Thermo-Diffusion with FEM Approach, *Symmetry* (2020), 12, 234, pp.1-15, doi:10.3390/sym12020234, www.mdpi.com/ journal/symmetry

[5]. Beg OA, Mabood F and Nazrul Islam M. : Homotopy simulation of nonlinear unsteadyrotating nanofluid flow from a spinning body. *International Journal of Engineering Mathematics* (2015); Article ID 272079, 15 pages, http://dx.doi.org /10.1155/2015/272079.

[6]. Buongiorno J. : Convective transport in nanofluids, *ASME J. Heat Transfer*, V.128, (2006)pp. 240–250

[7]. Choi S.U.S., Siginer D.A., Wang H.P. : Enhancing Thermal Conductivity of Fluids with Nanoparticles, Developments and Applications of Non-Newtonian Flows, *The American Society of Mechanical Engineers, New York*, FED-vol. 231/MDvol. 66, (1995) pp. 99–105.

[8]. Dulal P, Hiranmony M. Effects of temperature-dependent viscosity and variable thermal conductivity on mhd non-Darcy mixed convective discusion of species over a stretching sheet. *J of Egy Math Soc.*V.22(2014):pp.123-133.

[9]. Eastman J.A., Choi S.U.S., Li S., Yu W., Thompson L.J. : Anomalously increased effective thermal conductivity ofethylene glycol-based nanofluids containing copper nanoparticles, *Appl. Phys. Lett.* V.78, (2001)pp. 718–720.

[10]. Gayathri : Impact of Variable Viscosity, Activation Energy on MHD Mixed convective Heat and Mass Transfer Flow of a Nanofluid in a Cylindrical Annulus, *YMER*, Vol.21 : Issue 4 ((April) – 2022), pp. 211-223, ISSN : 0044-0477, http://ymerdigital.com

[11]. Hamad M.A.A, Pop. I, Unsteady MHD free convection flow past a vertical permeable flat plate in a rotating frame of reference with constant heat source in a nanofluid, *Heat Mass Tran. (*2011) vol.47, pp:1517–1524

[12]. Kiran Kumar T, Srinivasa Rao P, Shamshuddin Md : Effect of thermal radiation on nonDarcy hydromagnetic convective heat and mass transfer flow of a water–SWCNT's and MWCNT's nanofluids in a cylindrical annulus with thermo-diffusion and chemical reaction, International Journal of Modern Physics.B (2023) doi/10.1142/S0217979224500115

[13]. Mahajan A and Arora M. : Convection in rotating magnetic nanofluids. *Applied Mathematics and Computation*; V.219: (2013) pp..6284–6296.

[14]. Mohyud-Din, S.T.; Khan, U.; Ahmed, N.; Rashidi, M.M. A study of heat and mass transfer on magnetohydrodynamic (MHD) flow of nanoparticles. *Propuls. Power Res.* (2018), 7, 72–77

[15]. Mustafa, M.; Hayat, T.; Alsaedi, A. Axisymmetric flow of a nanofluid over a radially stretching sheet with convective boundary conditions. *Curr. Nanosci*. (2012), 8, 328–334.

[16]. Nadeem S and Saleem S. : Unsteady mixed convection flow of nanofluid on a rotating cone with magnetic field. *Appl. Nanoscience*; V.4: (2014) pp.405-414.

[17]. Oztop H. F. and Abu-Nada E., "Numerical study of natural convection in partially heated rectangular enclosures filled with nanofluids," *International Journal of Heat and Fluid Flow*, vol. 29, no. 5, (2008)pp. 1326–1336.

[18]. Patakota Sudarsana Reddy, P. Sreedevi, Ali J. Chamkha : MHD convective flow of swcnts-water and mwcnts-water nanofluid over a vertical cone with thermal radiation and chemical reaction, Journal of Porous Meida, Volume 26, Issue 7, 2023, pp. 47-68, DOI: 10.1615/JPorMedia.2022028664

[19]. Rana P, Bhargava R and Beg O.A. : Finite element simulation of unsteady magnetohydrodynamic transport phenomena on a stretching sheet in a rotating nanofluid. *Proc. I Mech. E- Part N: J. Nano materials, Nanoengineering and Nanosystems*, V.227: (2013)pp.77–99.

[20]. Sheikholeslami M, Hatami M and Ganji DD. : Nanofluid flow and heat transfer in a rotating system in the presence of a magnetic field. *J. Molecular Liquids*; V.190: (2014) pp.112–120

[21]. Sreedevi G and Prasada Rao D.R.V. "Effect of Dissipation and Radiation on Convective Heat Transfer Flow of a Rotating Cu-Water Nano-fluid in a Vertical Channel", International Journal for Research and Development in Technology (IJRDT), Vol. 8(2) (2017) pp. 21-30

[22]. Wang X, Xu X, Choi S.U.S. : Thermal conductivity of nanoparticle fluid mixture, *J. Thermophys. Heat Transfer*, V.13, (1999) pp.474–480.